Kinetic and Dynamic Study of Liquid–Liquid Extraction of Copper in a HFMC: Experimentation, Modeling, and Simulation

M. Younas, S. Druon-Bocquet, and J. Sanchez
Institut Européen des Membranes, UMR 5635, CNRS, ENSCM, UMII, Université de Montpellier II, CC 047, 2 Place Eugène Bataillon, 34095 Montpellier cedex 5, France

DOI 10.1002/aic.12076
Published online October 28, 2009 in Wiley InterScience (www.interscience.wiley.com).

In this work, we present the dispersion-free liquid–liquid extraction of copper from aqueous streams in a hollow fiber membrane contactor (HFMC). Copper has been transferred from aqueous solutions to heptane using LIX 84-I (2-hydroxy-5-nonylacetephenone oxime) as extracting agent. In a first step, batch experiments have been performed to identify the extraction kinetics and to measure the partition coefficient of copper aqueous-organic phase system. Then, the continuous recycled-base extraction process has been performed in a HFMC Liqui-Cel® module. The module has been modeled from resistance in series concept to gain the exit concentrations, which are used to develop a dynamic model to calculate the exit concentration of copper from the output of storage tanks. The model has been validated with experimental data at various operating conditions. The integrated process model algorithm was scripted in MATLAB® 7.4 R (a). Simulations have been made for a range of different operating parameters to determine the optimum criterion conditions. © 2009 American Institute of Chemical Engineers *AIChE J,* 56: 1469–1480, 2010
Keywords: copper extraction, HFMC, dynamic modeling, simulation

Introduction

Copper, a metal that people have used since early ancestors found shiny pieces of it among riverbed stones, became the basis of metallurgy because of its early extraction. The use of copper in farming and construction tools or electrical and electronic products is increasing its demand to develop new techniques for extraction.[1] Heavy metal-bearing water pollution was being a worldwide concern for the last few decades. Waste streams from metal plating industries, electrorefining industries, mining wastes, fertilizer industry, paints and pigments, and municipal or storm water runoff are threats to aqueous environment.[2–4] Liquid–liquid extraction of copper entails contacting aqueous solutions with liquid organic extractants causing extraction of Cu^{2+}. Organic extractants (hydroxyoximes) such as ketoximes (e.g., LIX 84 I) are found to be active in metal extraction.[5]

Environmental concerns, the increasing cost and scarcity of water, and decreasing price of membranes and their commercialization switch the tedious or time-consuming traditional solvent extraction technique over the membrane separations. Membrane separation has reduced the copper extraction from three stages, in early days, to a single stage. Furthermore, environmental impact should be less important.[6–8]

Liquid membranes such as emulsion liquid membranes (ELMs) and supported liquid membranes (SLMs) are in place for active extraction of heavy metals including copper. Many researchers have been found to use ELM and SLM for metal extraction with various organic extractants including LIX reagent.[9–12] Although these techniques, as a novel method of extraction, are considered for high membrane flux, destabilization of the membrane, complexity of the process, organic loss, and concerns over the osmotic transport

Correspondence concerning this article should be addressed to M. Younas at younas@iemm.univ-montp2.fr. or engr_unas@yahoo.com.

© 2009 American Institute of Chemical Engineers

of water across the membrane are the causes of operational difficulties.[6,11] Parallel to aforementioned techniques, nondispersive membrane extraction is a very simple hollow-fiber membrane-based liquid–liquid extraction process, which allows the circulation of the two phases through, for example, aqueous phase or organic phase either in shell or in tube side of the hollow fiber membrane contactor (HFMC). The membrane separates both phases and thus eliminates equilibrium limitations, high efficiency is obtained and organic loss can be reduced.[13,14] HFMC-based separation units are very compact and energy efficient. Fast mass transfer is achieved compared to conventional extraction units. For example, 600 times faster liquid extraction results than in mixer settlers due to large surface area per volume, 100 times bigger than in conventional extractors without direct mixing of the aqueous and organic phases, with no need for a difference in phase densities and with no problems due to loading and flooding.[15–17]

As far as the mass transfer of copper extraction is concerned, this field has received increasing attention in recent years. Mathematical modeling and study of characteristic parameters of HFMC to predict the performance of membrane solvent extraction of heavy metals have been widely investigated by researchers. Yun et al.[18] studied the copper extraction with LIX 84, and a mass transfer model of hollow fiber module was developed. Similar related work on nondispersive solvent extraction has been studied by Kumar et al.,[19] Juang and Huang,[20] Juang et al.,[21] and Lin and Juang.[22]

However, with introduction of new extractants with modified transport characteristics and novel techniques of nondispersion liquid–liquid extraction in HFMC, there is a necessity of developing new robust integrated dynamic models to study the mass transfer behavior under continuous unsteady state conditions, and hence, more computational work is required to bridge the algebraic and differential equations.

In this work, we explored, theoretically and experimentally, the dispersion-free extraction of copper ions from aqueous medium of sulfate solution with an organic extractant LIX 84-I diluted in *n*-heptane in a baffle-less HFMC mini module. The aim was to develop an integrated mathematical model of the recycled-based pilot plant after measuring the kinetics for batch extractive experiments. Once the model was validated with experimental data of dispersion-free extraction in HFMC, the influence of operating and process parameters was studied to get optimum conditions.

Materials and Methods

Reagents

The feed solution is an aqueous solution of Cu^{2+} prepared by dissolving analytical reagent grade $CuSO_4.5H_2O$ (purchased from Fisher scientific) in deionized water. The initial concentration of Cu^{2+} ranges from 1.5 to 31.5 mol m^{-3}. The extractant LIX 84-I (kindly provided by Cognis), a fluid amber liquid, is 2-hydroxy-5-nonylacetephenone oxime with a high flash point hydrocarbon diluent (kerosene) but the active LIX 84-I (oxime) concentration is 1.54×10^{-3} mol m^{-3} (45.34 mol %).[23] As shipped LIX 84-I was further diluted in *n*-heptane in various concentrations ranging from 77 to 308 mol m^{-3} to get the extracting organic phase.

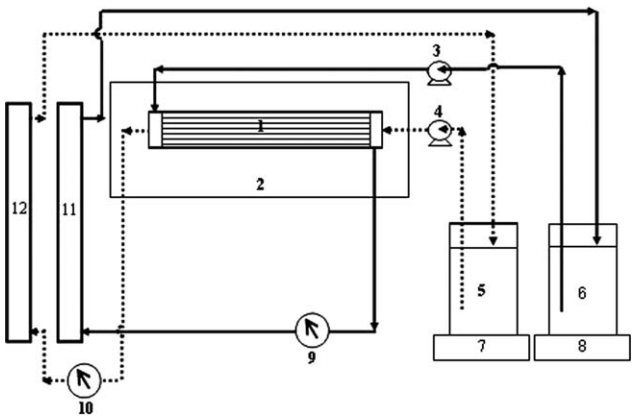

Figure 1. Schematic representation of experimental set up for dispersion-free liquid–liquid extraction in HFMC.

————, aqueous phase flow; ▪▪▪▪▪▪▪▪▪▪, organic phase flow; (1) HFMC; (2) constant temperature bath; (3), (4) pumps; (5), (6) storage tanks; (7), (8) stirrers; (9), (10) pressure gauges; (11), (12) rota meters.

Partition coefficient and kinetics

The calculation of partition coefficient is the first step in mass transfer model of liquid–liquid extraction. It is also important to know about the extent of copper extraction with LIX 84-I. Equal volume (25×10^{-6} m^3) of aqueous and organic phases of known concentrations were mixed in a thermostatic closed-type glass bottle at temperature (298 K) and were agitated by a magnetic stirrer at 1100 rpm for at least 45 min. The emulsified mixture was then placed overnight to achieve equilibrium. Copper concentration, initial and equilibrium after decantation, was analyzed with Varian atomic absorption spectrophotometer (Model FS 220). The pH of the aqueous phase was measured by pH meter. Similar experiments were done for initial copper concentration of 1.3–22.6 mol m^{-3} and oxime concentration of 77–308 mol m^{-3}. The temperature was kept constant at 298 K throughout the experiment. Each experiment was repeated three times and the mean value was considered. A good level of precision was found among the results.

HFMC module and experimental setup

Figure 1 shows the experimental setup used for liquid–liquid extraction. The main components of the pilot plant are storage tanks for aqueous and organic phases, stirrers and heaters, pumps, pressure gauges, flow meters, and HFMC module. The macroporous hollow fiber module used for liquid–liquid extraction was the Hoechst Celanese Liqui-Cel^{TM} X-50 1.7 × 5.5 mini module membrane contactor. The small size of the without baffle module basically designed for gas–liquid extraction could be used for limited use of liquid–liquid extraction. Additional information about this module is listed in Table 1.

Nondispersive copper extraction was made in HFMC, where copper-bearing aqueous phase was contacted with organic phase of LIX 84-I in *n*-heptane. Each phase was taken in the individual storage tanks. The volumes were fixed constant throughout the experiments, which are either 1 or

Table 1. Characteristics of HFMC Liqui-Cel™ X-50 1.7 × 5.5 Mini Module (Provided by Manufacturer)

Porosity (%)	40
Internal diameter of fibers (m)	2.2×10^{-4}
External diameter of fibers (m)	3×10^{-4}
Mean pore diameter (m)	4×10^{-8}
Active surface area (m^2)	0.58
Number of fibers	7400
Length of module shell (m)	121.8×10^{-3}
Diameter of shell (m)	42.5×10^{-3}

2×10^{-3} m^3 and 1×10^{-3} m^3 for aqueous and organic phase, respectively. The membrane contactor module was placed horizontally in constant temperature bath to ensure the temperature at 298 K. The storage tanks were also placed on heating source to keep the inside fluid temperature constant at 298 K. Both fluids were constantly agitated by magnetic stirrer. The temperature is kept constant at ambient room temperature (298 K) because equilibrium condition of the reaction and so as the partition coefficient is affected by temperature, and these effects are indispensable to consider in mass transfer modeling. However, work is undertaking to consider all these sensitivities. Rotameters, control valves, and pressure gauges were used to control flow rates and pressure across the membrane contactor module. A positive pressure of 0.3–0.6 bar was ensured on aqueous phase side of fibers; however, transmembrane pressure difference between the fluids has shown no effect on mass transfer.[16] Before experiments, organic phase and deionized water were introduced into the module for at least 30 min or till the stabilization of the parameters. The deionized water phase was then suddenly replaced by copper-bearing aqueous phase solution. At this moment, the extraction of copper starts from aqueous phase to organic phase. Aqueous phase samples of $\sim 2 \times 10^{-6}$ m^3 were taken at various time intervals. The samples were analyzed using atomic absorption to evaluate the copper concentration. Copper concentration in organic phase was calculated by mass balance. The aim of dispersion-free copper extraction in HFMC was to validate the dynamic mass transfer model; hence, the experiments were repeated, in the similar manner, for different operating conditions.

Mass Transfer Modeling

Estimation of mass transport properties

Density and viscosity of organic phase, diffusion coefficient of copper ions in aqueous phase, and Cu^{2+}-oxime complex in organic phase are important characteristics to be estimated. The diffusion coefficient of copper ions in the aqueous phase was calculated with Hayduk and Minhas estimation correlation.[24]

$$D_{A,B} = 1.25 \times 10^{-8}\left(\upsilon_A^{-0.19} - 0.292\right)T^{1.52}\eta_B^{\gamma} \tag{1}$$

$$\gamma = \frac{9.58}{\upsilon_A} - 1.12 \tag{2}$$

The subscripts A and B represent Cu^{2+} and water, respectively. υ_A is the molar volume of solute A at its normal boiling point (cm^3 mol^{-1}), T is the temperature in Kelvin, and η_B is the dynamic viscosity of water (cP).

Hayduk and Minhas correlation[24] for nonaqueous solutes in nonelectrolytes was used to estimate the diffusion coefficient of Cu^{2+}-oxime complex in the organic phase.

$$D_{A,B} = \frac{1.55 \times 10^{-8}T^{1.29}\left(\pi_B^{0.5} \Big/ \pi_A^{0.42}\right)}{\eta_B^{0.92}\upsilon_B^{0.23}} \tag{3}$$

The subscripts A and B denote copper complex and organic phase, respectively. π_A and π_B are parachors for the solute and solvent, respectively, and υ_B is the molar volume of organic phase (m^3 mol^{-1}). η_B is the dynamic viscosity of organic phase (cP) and was calculated by the method of Grunberg and Nissan[24] in 1949.

Reaction kinetics of copper extraction

Although the pioneering work on the extraction kinetics of copper with LIX 65N was published by Flett et al.,[25] the complexation of copper ion by ketoximes has been studied by many researchers.[26,27] The reaction is shown in general form, schematically and stoichiometrically as;

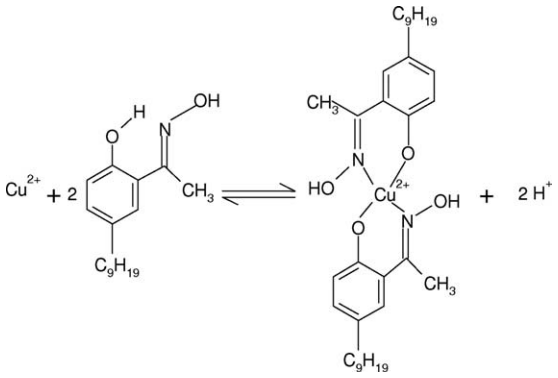

$$Cu^{2+} + 2\,\overline{HR} \rightleftharpoons \overline{CuR}_2 + 2\,H^+;\ \kappa_{ex}, \tag{4}$$

where HR and CuR_2 represent the oxime and copper-oxime complex, respectively, while over bar shows the organic phase. κ_{ex} is the extraction equilibrium constant and can be shown by the following equilibrium relationship.

$$\kappa_{ex} = \frac{C^{\overline{CuR}_2}.\left(C^{H^+}\right)^2}{C^{Cu^{2+}}.\left(C^{\overline{HR}}\right)^2}, \tag{5}$$

where C is denoted for concentration and superscript shows the ionic specie. The partition coefficient of a component between two phases is the ratio of the component concentration in organic phase to component concentration in aqueous phase at equilibrium and is shown by the following relationship,

$$P = \frac{C_{eq}^{\overline{CuR}_2}}{C_{eq}^{Cu^{2+}}} = \frac{C_{ini}^{Cu^{2+}} - C_{eq}^{Cu^{2+}}}{C_{eq}^{Cu^{2+}}} \tag{6}$$

$$\log\ P = \log\ \kappa_{ex} + 2\ \log\frac{C^{\overline{HR}}}{C^{H^+}}. \tag{7}$$

It is evident that copper loss in aqueous phase is transferred to organic phase, hence making copper mole balance across the storage tanks gives:

$$V_{aq}\left(C_{ini}^{Cu^{2+}} - C^{Cu^{2+}}\right) = V_{org}\left(C^{\overline{CuR}_2} - C_{ini}^{Cu^{2+}}\right) \tag{8}$$

as initially there is no copper in the organic storage tank;

$$C^{Cu^{2+}} = C_{ini}^{Cu^{2+}} - R_v.C^{\overline{CuR}_2} \tag{9}$$

$$\text{where}\ \ R_v = \frac{V_{org}}{V_{aq}} \tag{10}$$

$$\frac{C^{Cu^{2+}}}{C_{ini}^{Cu^{2+}}} = 1 - R_v.\frac{C^{\overline{CuR}_2}}{C_{ini}^{Cu^{2+}}}. \tag{11}$$

In the similar way, mole balance for extractant (LIX 84-I) means the transfer of oxime from its initial concentration to a certain concentration of copper-oxime complexant in the organic phase storage tank;

$$C_{ini}^{\overline{HR}} + C^{\overline{HR}} = 2.C^{\overline{CuR}_2} \tag{12}$$

$$1 - \frac{C^{Cu^{2+}}}{C_{ini}^{Cu^{2+}}} = \frac{R_v}{C_{ini}^{Cu^{2+}}}.\frac{C_{ini}^{\overline{HR}} - C^{\overline{HR}}}{2} \tag{13}$$

$$\Phi = \frac{R_v}{2}.\frac{C_{ini}^{\overline{HR}}}{C_{ini}^{Cu^{2+}}}.\left(1 - \frac{C^{\overline{HR}}}{C_{ini}^{\overline{HR}}}\right) \tag{14}$$

$$\text{as}\ \ \Phi = 1 - \frac{C^{Cu^{2+}}}{C_{ini}^{Cu^{2+}}} \tag{15}$$

is the extraction efficiency defined as the ratio of copper concentration transferred from aqueous phase to organic phase to the initial concentration of copper in aqueous phase. Combination of Eqs. 6 and 15 gives result to the following equation,

$$\Phi = \frac{P}{1+P}. \tag{16}$$

Equations 6–12 are sufficient to calculate experimentally the partition coefficient and equilibrium extraction constant, whereas Eqs. 14 and 16 show how the various parameters affect the extraction efficiency and partition coefficient. Furthermore, these equations guide us to optimize the different parameters to achieve the maximum extraction, though these equations are not able to simulate the results.

Steady-state mass transfer model in HFMC

During the last decades, new various types of membrane contactors have been introduced, and mathematical model was built to predict the performance of liquid–liquid extraction for various applications.[28] Here, Liqui-Cel™ X-50, 1.7 × 5.5 mini module membrane contactor is used to model liquid–liquid extraction. It is based on the use of hollow fibers bundle of cylindrical geometry inserted in a polycarbonate casing. The pores of the fibers are filled with the organic phase so far as the fibers are hydrophobic. Aqueous feed phase is chosen to flow outside the fibers, for example, in the shell of the contactor because this configuration offers a larger exchange area than the fiber-feed configuration,[29] although Breembroek et al.[30] reported a lower permeability for the shell side aqueous feed flow than that for the fiber side aqueous feed flow. A slight differential pressure across the membrane is necessary to stabilize the organic phase inside the pores of the membrane. The organic phase enters the hollow surface and then distributes uniformly into the fibers. After that it flows in the fibers throughout the module from one end to the other. On the other hand, the aqueous phase enters on one side of the shell and flows to the other end counter currently. It was assumed that the fluid in the shell side flows parallel to the fiber tubes, and each fiber is surrounded by a certain area of shell side fluid. This surrounded area is called as "flow cell" (see Figure 2); therefore, the number of flow cells are equal to the number of fibers. It is further assumed that the fibers are arranged in the ring starting from the single fiber in the first ring of the middle of the module and then increasing the number of fibers in the successive rings till the extremity of the shell.

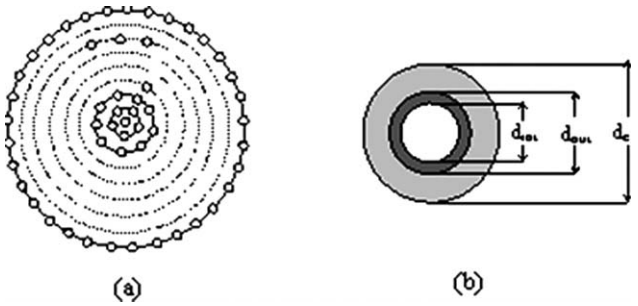

Figure 2. Representation of "flow cell" concept in the module.

(a) Fibers distribution in rings and (b) flow cell.

The following assumptions are necessary to consider for model development:

- The system works in steady-state and isothermal conditions,
- equilibrium is reached at the fluid-fluid interface,
- pore size and wetting characteristics are uniform throughout the membrane,
- the curvature of the interface neither significantly affect mass transfer, solute distribution nor interfacial area,
- fluids are completely immiscible,
- solute transport occurs only in the porous fraction of membranes,
- the partition coefficient of the solute is constant in the considered range of concentrations, for example, during one experiment, and
- the transfer of solute across the membrane is justified by the resistance in series model.

Parallel flow without-baffle HFMC module is divided into N_a axial segments and N_r radial rings as shown in Figure 3. The axial stage 1 corresponds to the entry of the feed, whereas the radial ring 1 corresponds to module's central ring. Similarly, the N_a shows the last stage and thus entry

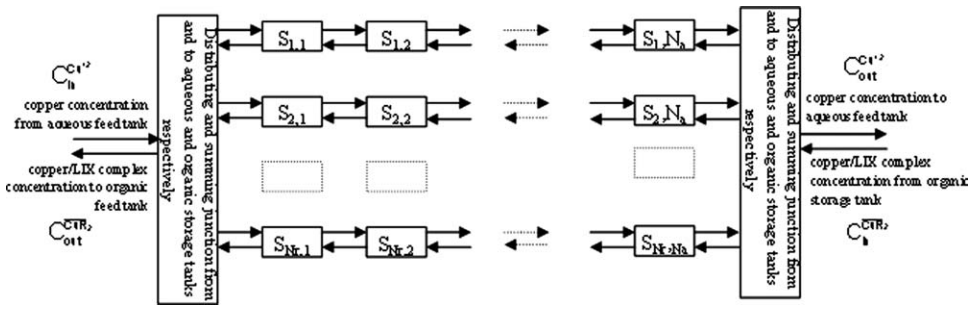

Figure 3. Schematic representation of axial and radial model of HFMC without baffle.

$S_{i,j}$ denotes a specific stage, where i and j holds for the specified ring and axial stage, respectively.

side of the solvent, whereas N_r points out the periphery of the module. One ring is considered to have only one fiber width. The calculations for the model development are based on the individual compartment. The stage $S_{nr,na}$ considered to be located in individual compartment is shown in Figure 4, where (nr, na) corresponds to the radial ring and axial division. A mathematical description of this system is based on resistances in series model and mass transfer equations in the axial/radial direction, and the equation of continuity for the solute. The concentration profile of solute and oxime transfer across the porous membrane is shown in Figure 5. Membrane-based liquid–liquid extraction is a concentration-driven operation and the whole process can be explained by Fick's law of diffusion. Solute transfer across the membrane is defined by the following steps:

• Diffusion of copper ions (Cu^{2+}) in the aqueous phase (shell side) from the bulk to aqueous-organic interface through the aqueous boundary layer,

$$J_1 = k_{aq}\left(C_1^{Cu^{2+}} - C_2^{Cu^{2+}}\right) \tag{17}$$

• equilibrium at aqueous-organic interface, the reaction of Cu^{2+} in aqueous phase with oxime ($\overline{HR}$) in organic phase to form Cu^{2+}-oxime complex ($\overline{CuR_2}$),

$$C_3^{\overline{CuR_2}} = P.C_2^{cu^{2+}} \tag{18}$$

• diffusion of Cu^{2+}-oxime complex ($\overline{CuR_2}$) from the aqueous-organic interface to the inside of fiber wall through the organic phase filled pores,

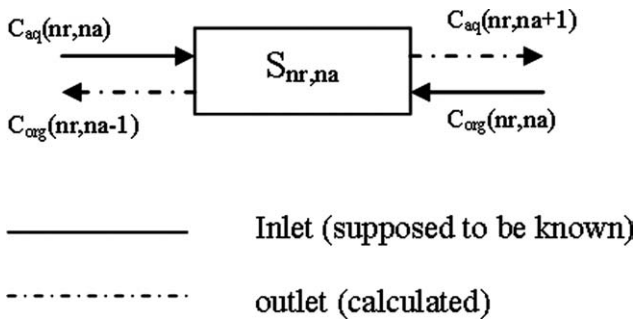

Figure 4. Representation of stage $S_{nr,na}$.

C_{aq} and C_{org} exhibit the solute concentrations in aqueous and organic phase, respectively.

$$J_2 = k_{mb}.\left(C_3^{\overline{CuR_2}} - C_4^{\overline{CuR_2}}\right) \tag{19}$$

• diffusion of Cu^{2+}-oxime complex ($\overline{CuR_2}$) from the inside of fiber wall to the organic phase bulk (fiber side),

$$J_3 = k_{org}.\left(C_4^{\overline{CuR_2}} - C_5^{\overline{CuR_2}}\right). \tag{20}$$

Steady-state Cu^2 and $\overline{CuR_2}$ balance equations on aqueous and organic side of the module, respectively, are shown as follows,

$$J^{Cu^{2+}} = Q_{aq}.\left(C_1^{Cu^{2+}} - C_{out}^{Cu^{2+}}\right) = Q_{aq}.\left(C_{in}^{Cu^{2+}} - C_{out}^{Cu^{2+}}\right) \tag{21}$$

$$J^{\overline{CuR_2}} = Q_{org}.\left(C_{out}^{\overline{CuR_2}} - C_5^{\overline{CuR_2}}\right) = Q_{org}.\left(C_{out}^{\overline{CuR_2}} - C_{in}^{\overline{CuR_2}}\right). \tag{22}$$

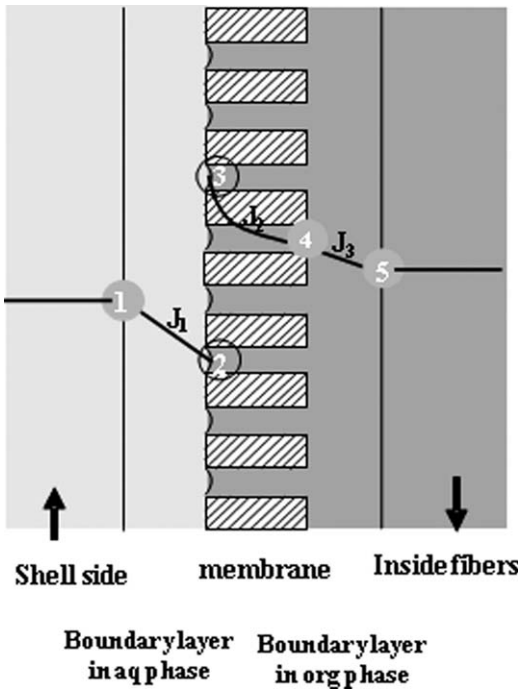

Figure 5. Concentration profile across HFMC.

(1) C_1, (2) C_2, (3) C_3, (4) C_4, and (5) C_5.

Pseudo-steady state holds the following equalities,

$$J_1 = J_3 = J_5 = J^{Cu^{2+}} = J^{\overline{CuR}_2}, \tag{23}$$

where Q_{aq} and Q_{org} are volumetric flow rates of aqueous feed and organic solvent phases (known); $C_{in}^{Cu^{2+}}$ and $C_{in}^{\overline{CuR}_2}$ are the initial concentrations of copper ion and Cu^{2+}-oxime complex entering the contactor module (known); $C_{out}^{Cu^{2+}}$ and $C_{out}^{\overline{CuR}_2}$ are the final concentrations of copper ion and Cu^{2+}-oxime complex leaving the module (to be calculated); k_{aq}, k_{mb}, and k_{org} represent the individual mass transfer coefficients of the respective components "on aqueous side (shell side)," "on membrane side," and "on solvent side (fiber side)," respectively. Shell side mass transfer coefficient depends on the hydrodynamics, geometry of the module, number of fibers, and the presence of baffle. In our case, we used the following correlation based on liquid–liquid extraction with various solutes and solvents for parallel flow without baffle[18]:

$$Sh_{aq} = \beta[d_h(1-\theta)/L]Re^{0.60}.Sc^{0.33}, \tag{24}$$

where θ is the packing fraction, d_h is the hydraulic diameter, L is the fiber length, and β is a constant equal to 5.85 and 6.1 for hydrophobic and hydrophilic membranes, respectively, in the range of $0 < Re < 500$ and $0.04 < \theta < 0.4$. Sh, Re, and Sc stand for Sherwood number, Reynolds number, and Schmidt number, respectively.

The transmembrane mass transfer coefficient is simply a characteristic of a diffusion mechanism through a solvent-filled porous medium. Thus, membrane side mass transfer coefficient depends on the membrane structure and solute diffusion coefficient and is given by the following equation for organic fluid-filled pores[16];

$$k_{mb} = \frac{D_{org}.\varepsilon}{\sigma.\tau}. \tag{25}$$

D_{org} is the diffusion coefficient of Cu^{2+}-oxime complex in organic phase, which fills the membrane pores. Tortuosity is the function of porosity of membrane and their relationship depends upon the pore geometry. For loose-packed membrane pore structure, we consider the Wakao-Smith relationship,[15,19]

$$\tau = 1/\varepsilon. \tag{26}$$

Similarly the modified Léveque equation is used to describe the correlation to estimate the mass transfer coefficient in tubes of the cylindrical hollow fiber, as reported by many researchers[31];

$$Sh_{org} = 1.62(Gz)^{1/3} \quad \text{for } Gz \geq 6 \tag{27}$$

$$Sh_{org} = 0.5(Gz) \quad \text{for } Gz \leq 6. \tag{28}$$

Gz and Sh are Greatz and Sherwood numbers. The dimensionless numbers are defined as

$$Sh = \frac{k.d}{D} \tag{29}$$

$$Gz = Re.Sc.\frac{d}{L} \tag{30}$$

$$Re = \frac{d.v.\rho}{\eta} \tag{31}$$

$$Sc = \frac{\eta}{\rho.D}. \tag{32}$$

Overall mass transfer coefficient is measured from local mass transfer coefficients estimated at aqueous feed side, membrane side, and solvent side. The expression for the overall mass transfer coefficient for a hydrophobic membrane with the aqueous phase flowing on shell side, the driving force based on the aqueous phase concentration, and with no chemical reaction, described by several researchers[32] is as follows:

$$\frac{1}{K_{aq}} = \frac{1}{k_{aq}} + \frac{d_{ext}}{P.k_{mb}.d_{lm}} + \frac{d_{ext}}{P.k_{org}.d_{int}} \tag{33}$$

The resistance to mass transfer is the sum of the individual mass transfer resistance on aqueous side (R_{aq}), across membrane (R_{mb}), and on organic side (R_{org}), which are first, second, and third terms on right side of Eq. 33, respectively.

Mass transfer dynamic model across storage tank

Starting from the initial known concentrations in the storage tanks, the aqueous and the organic phases are continuously recycled after passing through the contactor module. Therefore, copper is extracted every time both phases are in contact in membrane pores and is rediluted every time when remixed within storage tank. Interest has been taken to calculate the copper concentration variation within/at the exit of the aqueous phase storage tank. Resistance in series model takes the known concentrations from storage tanks and gives the outlet concentration at the other end of module. The fluid with new concentrations re-enters the storage tanks. The storage tanks are taken as ideally mixed units and are kept at isothermal conditions. The dynamic model developed in a previous work[33] has been used to calculate the copper concentration within the storage tank at time $t + \Delta t$.

$$C_{in}^{Cu^{2+}}(t+\Delta t) = \frac{\Delta t}{\Gamma_{aq}}.C_{out}^{Cu^{2+}}(t) + C_{in}^{Cu^{2+}}(t).\left[1 - \frac{\Delta t}{\Gamma_{aq}}\right] \tag{34}$$

$$\text{where } \frac{V_{aq}}{Q_{aq}} = \Gamma_{aq} \tag{35}$$

$C_{in}^{Cu^{2+}}(t)$ and $C_{out}^{Cu^{2+}}(t)$ are copper concentrations at the inlet and exit of the module at time t, respectively, where V_{aq} is the volume of aqueous phase storage tank. The copper-oxime complex concentration in organic phase storage tank at any time can be calculated from Eq. 9.

Results and Discussion

Mass transport properties

The calculated value of diffusion coefficient of copper ions in aqueous phase was 2.79×10^{-9} m^2 s^{-1} at 298 K, which is close to the values calculated by Hu and

Table 2. Transport Properties and Diffusion of Cu^{2+}/Oxime Complex in Organic Phase at 298 K

% v/v LIX 84-I	ρ (kg m^{-3})	η (kg m^{-1} s^{-1})	$D_{Cu^{2+}\text{-oxime complex}}$ (m^2 s^{-1})
5	672	0.46×10^{-3}	1.18×10^{-9}
10	680	0.52×10^{-3}	1.05×10^{-9}
15	689	0.60×10^{-3}	9.30×10^{-10}
20	698	0.69×10^{-3}	8.20×10^{-10}
100	900	3.36×10^{-3}	1.90×10^{-10}

Wienceck.[34] In contrast, it was not easy to estimate the diffusion coefficient of Cu^{2+}-oxime complex in organic phase. Actually, the as shipped LIX 84-I was the mixture of active LIX component (oxime) and kerosene. This mixture (LIX 84-I) was further diluted in *n*-heptane from 5 to 20 % v/v, thus the organic phase consists of three components, for example, oxime, kerosene, and *n*-heptane. Cognis provided the values of density and kinematic viscosity (at 313 K) as 900 kg m^{-3} and 2.71×10^{-3} m^2 s^{-1} (2.44 cP), respectively. Lewis-square equation was used to re-estimate the viscosity at 298 K. Molar volumes of oxime, kerosene, and *n*-heptane are found to be 329, 278, and 161 cm^3 mol^{-1}, respectively, by the Schroder group additive method, whereas parachors for Cu^{2+}-oxime complex, oxime, kerosene, and *n*-heptane are found to be 1611.4, 821.2, 511, and 297 cm^3 $g^{1/4}$ $s^{-1/2}$, respectively, by Qyayle group contribution method.[14,24] As various LIX 84-I concentrations from 5 to 20 % v/v are used for copper extraction, the effects of transport properties on the calculation of diffusion coefficient of Cu^{2+}-oxime complex in organic phase were taken into account and summarized in Table 2. Breembroek et al.[30] in their work suggested that diffusion coefficient of copper complex in the organic phase should be greater than 1×10^{-11} m^2 s^{-1} who studied copper extraction using LIX 84-I in a hollow fiber SLMs.

Partition coefficient and extraction kinetics

The speed of reaction between copper-carrying aqueous phase and LIX 84-I-carrying organic phase was measured and shown in Figure 6. Copper concentration varies from 1.3 to 22.6 mol m^{-3} at constant oxime concentration of 77 mol m^{-3} in organic phase. It is shown that the reaction is fast at the interface and completes in almost 2 min though extraction becomes faster at lower copper concentration. It explains that reaction is instantaneous at the interface and does not offer resistance in mass transfer of copper through membrane interface. As a basic parameter for mass transfer model, partition coefficient of copper with oxime was measured experimentally by batch extraction. The values of partition coefficient calculated by this way are used to find the equilibrium extraction constant; detailed data have been tabulated in Table 3. Equilibrium extraction constant, from log *P* vs. log C^{HR}/C^{H} graph, could be found for various oxime concentrations. The slope of each line achieved as "2" verifies the experimental data with the kinetic equation (not shown graphically). Table 3 shows that partition coefficient decreases with the increase of initial copper and vice versa with oxime concentration. The change is remarkable at the point of copper concentration equal to 15.75 mol m^{-3}. The increase in partition coefficient is higher when copper concentration decreases below 15.75 mol m^{-3} and when oxime concentration varies from 77 to 308 mol m^{-3}, but change is not significant when copper initial concentration increases above 15.75 mol m^{-3} at all values of oxime concentration.

Process model validations

Mass transfer model, discussed in section "mass transfer modeling," was integrated with the transient equation (44). Integrated model was then scripted in MATLAB® 7.4 R (a) and run by simulation to predict the decrease of copper concentration in the aqueous phase storage tank in function of time. Two different values of operating parameters were chosen to simulate the model. For example, partition coefficient values of 28 and 120 with aqueous phase flow rates of 11.1×10^{-6} and 9.7×10^{-6} m^3 s^{-1} as well as with 1:1 and 2:1 volume ratios of aqueous and organic phases, respectively, were applied. Following the same operating parameters, the experiments were performed for dispersion-free extraction of copper in HFMC over the span of time, and experimental data were compared with the simulated results. For example, the comparison between experimental and model data is given in Figure 7. It was found that, over various run of experiments, model was validated with experimental data at a very good level of accuracy. Experimental error of ±5% is considered as tolerable. Furthermore, it is found that the extraction of copper is comparatively fast initially and then gradually slows down and eventually reaches to a stabilized value.

Model simulation

Once the model is validated, simulations were run to investigate the effect of various parameters on the extraction of copper. Dynamic behavior of relative copper concentration in aqueous phase storage tank was to be studied, which results the extraction efficiency, shown by Eq. 15, of the process at any time and stabilization time, defined in a previous work,[33] of the extraction process. Another important parameter concerning mass transfer is the overall mass transfer coefficient defined in Eq. 33, which was aimed to be calculated by simulation. This equation comprises the three

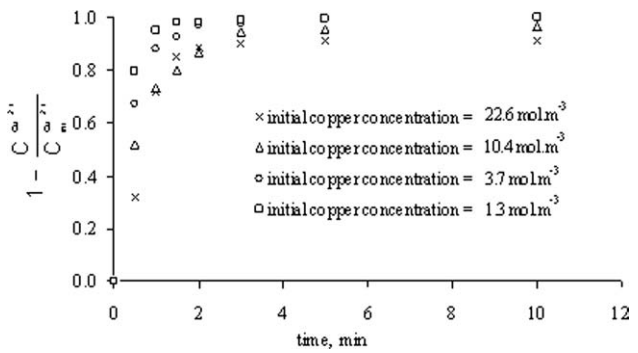

Figure 6. Copper extraction rate with 77 mol m^{-3} oxime concentration for various copper concentrations.

Table 3. Partition Coefficient of Copper with LIX 84-I in *n*-Heptane at 25°C

% v/v LIX 84-I in *n*-heptane	5			10			15			20		
C_{ini}^{HR} (Oxime Concentration) (mol m^{-3})	77			154			231			308		
Before Mixing	At Equilibrium											
$C_{ini}^{Cu^{2+}}$ (mol m^{-3})	Aq. Phase (pH)	$C_{eq}^{Cu^{2+}}$ (mol m^{-3})	P	Aq. Phase (pH)	$C_{eq}^{Cu^{2+}}$ (mol m^{-3})	P	Aq. phase (pH)	$C_{eq}^{Cu^{2+}}$ (mol m^{-3})	P	Aq. Phase (pH)	$C_{eq}^{Cu^{2+}}$ (mol m^{-3})	P
3.94	4.82	0.007	528	2.20	0.006	666	2.11	0.004	1041	2.17	0.003	1530
7.87	4.72	0.65	120	1.98	0.036	220	1.89	0.021	379	1.93	0.013	627
15.75	4.52	0.541	28	1.75	0.225	69.1	1.61	0.140	111	1.66	0.112	139
23.62	4.48	2.233	9.6	1.70	0.699	32.8	1.64	0.411	56.5	1.62	0.312	74.6
31.50	4.46	5.386	4.8	1.58	1.595	18.7	1.55	0.932	32.8	1.50	0.709	43.4

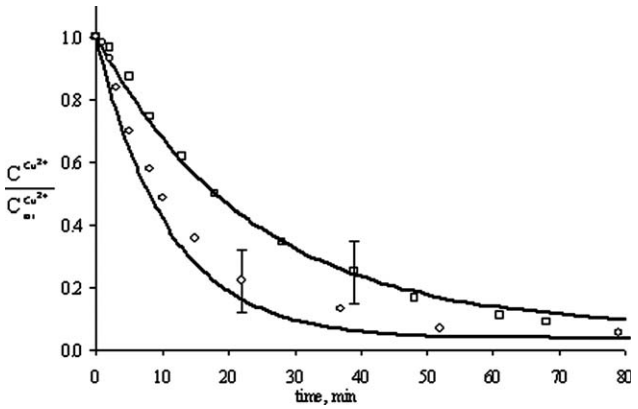

Figure 7. Comparison of model—simulated results (solid line) with experimental results (points).

(o): $P = 28$, $Re_{aq} = 7.1$, $Re_{org} = 8.0$, $V_{aq} = 1 \times 10^{-3}$ m^3, $V_{org} = 1 \times 10^{-3}$ m^3; (□): $P = 120$, $Re_{aq} = 6.2$, $Re_{org} = 7.7$, $V_{aq} = 2 \times 10^{-3}$ m^3, $V_{org} = 1 \times 10^{-3}$ m^3.

individual mass transfer resistances, for example, resistance on aqueous side, resistance within membrane, and resistance in organic side of the membrane, which were also simulated accordingly.

Effect of initial concentration of copper ions and LIX 84-I oxime

The initial concentration of copper ions is an important parameter to consider in extraction process. It is necessary to define the system of extraction whether it is the recovery of copper from aqueous wastes or extraction of copper in large quantities like in hydrometallurgy. In the former case, copper can be found in less concentration, whereas in the latter case higher copper concentrations are concerned in extraction process. Integrated model was used to simulate the effect of copper ion concentration with a fixed oxime concentration. Five arbitrary values of copper concentration were selected for the study ranging from 3.9 to 31.5 mol m^{-3} against a constant oxime concentration of 77 mol m^{-3}. It has been

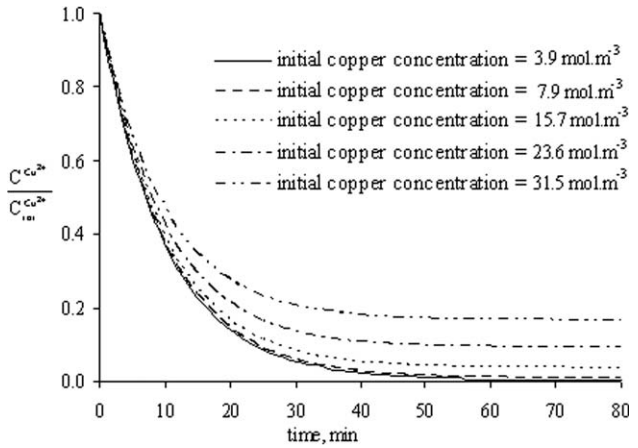

Figure 8. Effect of initial copper feed concentration on extraction dynamics with 77 mol m^{-3} oxime concentration.

$Q_{aq} = 12.5 \times 10^{-6}$ m^3 s^{-1}; $Q_{org} = 6.7 \times 10^{-6}$ m^3 s^{-1}.

found, from Figure 8, that copper concentration loss decreases with the increase of copper initial concentration. However, it is observed that the effect is nominal for copper initial concentration less than that of 7.9 mol m^{-3}. The calculated ultimate extraction efficiencies are 83, 91, and 96% for 31.5, 23.6, and 15.7 mol m^{-3}, respectively, of copper initial concentration. Almost all copper has been recovered from aqueous phase when copper initial concentration was 7.9 mol m^{-3} or less. Simulated results give the overall mass transfer coefficient values of 1.97×10^{-6}, 1.97×10^{-6}, 1.93×10^{-6}, 1.85×10^{-6}, and 1.75×10^{-6} m s^{-1} for copper initial concentration of 31.5, 23.6, 15.7, 7.9, and 3.9 mol m^{-3}, respectively.

We have found in a previous work[33] that initial concentration does not affect the extraction dynamics and solute (aroma compounds) extraction efficiency is same irrespective of initial feed concentration, which is contrary to our recent work. This difference can be explained with the fact that the initial aroma compound concentration in aqueous phase does not affect the partition coefficient; however, as discussed in section "partition coefficient and extraction kinetics" of this work, the partition coefficient changes remarkably with copper initial concentration.

In the similar manner, the effect of oxime initial concentration was also simulated. The oxime initial concentration was varied from 77 to 308 mol m^{-3} at constant copper initial copper concentration of 15.7 mol m^{-3}. It can be shown that copper extraction was little improved when oxime concentration in organic phase increases from 77 to 154 mol m^{-3}, but further increase of oxime concentration has no observable effect. Ultimate extraction efficiency remains between 96 and 99% for the selected range of oxime concentration. Furthermore, the effect on the initial velocity of extraction, related to magnitude of the gradient, is negligible. It should be known that, as discussed in section "Partition coefficient and extraction kinetics," the span of partition coefficient for the studied oxime concentration is between 28 and 139.

Breembroek et al.[30] showed that the extraction is independent of LIX 84-I concentration above 230 mol m^{-3} for copper extraction in hollow fiber SLM. Juang et al.[21] examined the dispersion-free copper extraction with a kerosene solution of di(2-ehtylhexyl)phosphoric acid in HFMC. In their mechanistic model, they showed that aqueous layer resistance increases with the decrease of copper initial concentration and increasing extractant concentration under specified conditions. Similarly, Hu and Wiencek,[34] in their work for emulsion-liquid-membrane copper extraction with LIX 84/kerosene in HFMC, indicated that predominant resistance lied in aqueous phase layer at very low copper and very high LIX 84 initial concentrations.

In this work, it is found that 88.6 to almost 100% resistance lies in aqueous phase layer when initial copper concentration decreases from 31.5 to 3.9 mol m^{-3}, respectively. Also, the aqueous layer dominates the overall mass transfer resistance, which is more than 98% for range of values studied here. Therefore, organic layer and membrane layer resistances are negligible but become significant at higher copper and lower extractant initial concentrations. The stabilization time is not affected by the initial copper and oxime concentration though the magnitude varies as 50 and 80 min, respectively, under the specified operating conditions.

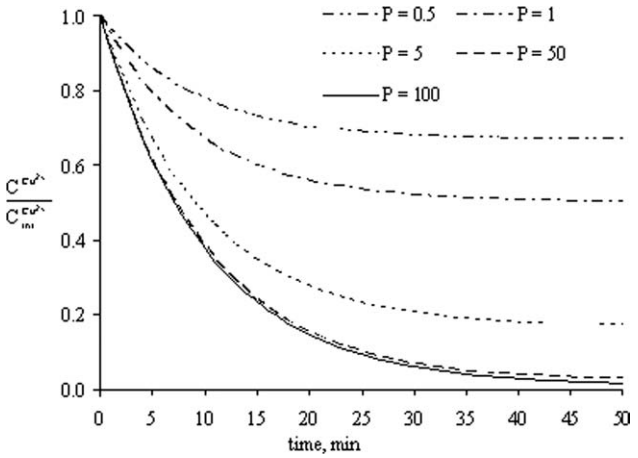

Figure 9. Effect of partition coefficient on extraction dynamics of copper with LIX 84-I.

Effect of partition coefficient

Partition coefficient is an important parameter of mass transfer model. It has been discussed in section "partition coefficient and extraction kinetics" that partition coefficient can be influenced by many parameters such as initial copper and oxime concentration, interest has been taken to study the effect of partition coefficient on liquid–liquid copper extraction in HFMC and on the dynamics of the plant.

Simulations were run for arbitrary values of partition coefficient of 0.5, 1, 5, 50, and 100 at aqueous and organic phase flow rates of 12.5×10^{-6} and 6.7×10^{-6} m^3 s^{-1}, respectively. The simulated effects were studied for a wide range of copper initial concentration, for example, 0.39, 15.7, and 78.7 mol m^{-3}, although oxime concentration was assumed constant at 77 mol m^{-3}. It can be observed, from Figure 9, that improved extraction is achieved with the increase of partition coefficient. Partition coefficient values of 0.5, 1, and 5 give the extraction efficiency of 33, 50, and 83%, respectively, but partition coefficient values of 50 and 100 result almost on same extraction efficiencies, for example, 97 and 98%, respectively. Partition coefficient also affects the overall mass transfer coefficient, which is 1.95×10^{-6} m s^{-1} for a partition coefficient equal to 100, which decreases to 0.77×10^{-6} m s^{-1} when the partition coefficient decreases to 0.5. Similarly, the aqueous phase resistance also decreases with the decrease of partition coefficient. Aqueous phase resistance decreases from 99 to 39% for the studied range of partition coefficient. It is worth noting that stabilization time remains same for all values of partition coefficient.

Therefore, change in partition coefficient affects the copper extraction irrespective of copper initial concentration, although it has been discussed, in section "effect of initial concentration of copper ions and LIX 84-I oxime," that copper initial concentration affects the extraction, whereas oxime initial concentration does not. This can be justified as partition coefficient can be modified by various other factors such as pH, temperature, and type of diluent without changing the initial concentration of copper and oxime. For example, Yun et al.[18] and Hu and Wiencek[35] studied the copper/LIX84-heptane and copper/LIX84-tetradecane system,

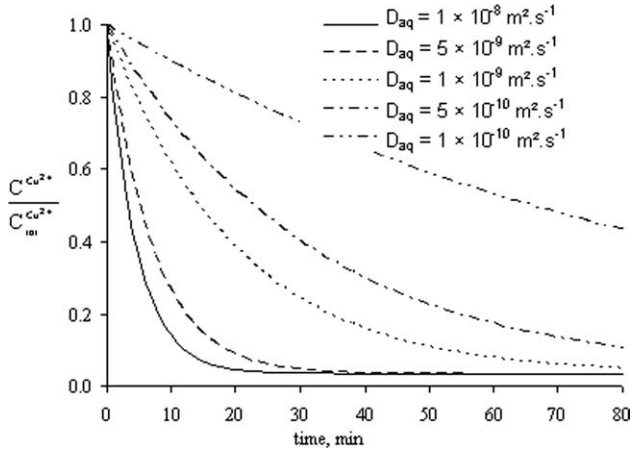

Figure 10. Effect of copper ions diffusion coefficient in aqueous phase on extraction dynamics of copper with LIX 84-I.

respectively, and obtained experimental values of partition coefficients under the same conditions of aqueous and organic phases. It was found that larger values of partition coefficient were achieved when tetradecane was used as a diluent in the later work. Similarly, other researchers[36,37] studied the effect of diluents on the extraction of copper with oxime extractant using several diluents. They found different values of extraction constant and diluent properties on the same conditions for various diluents. Furthermore, it has been found that the effect is not linear with partition coefficient, and effect is negligible for a partition coefficient greater than 50 under the specified condition, which supports the work discussed in our previous work.[33]

Effect of copper diffusivity in aqueous phase

Diffusion coefficient of copper in the aqueous phase is another important parameter to be studied. Solutes with improved values of diffusion coefficient ease the extraction process. The transport of solute near the membrane and within the pores relates to its diffusivity and, thus, is the only parameter taken into account to determine the mass transfer especially in laminar flow system, where the mass transfer coefficient is highly dependent on diffusion coefficient.[38] In addition to it, from Eq. 1 and Table 2, it is seen that diffusion coefficient of solute is affected by temperature and LIX 84-I concentration, respectively. Therefore, interest has been taken to define the limiting values of diffusion coefficient on copper extraction in HFMC. Five different values of copper diffusion coefficient in aqueous phase were chosen arbitrary, they are 1×10^{-8}, 5×10^{-9}, 1×10^{-9}, 5×10^{-10}, and 1×10^{-10} m^2 s^{-1}. Simulations are run to study the effect of copper loss for copper initial concentration of 15.7 mol m^{-3}, which corresponds to a partition coefficient of 28 against aqueous and organic phase Reynolds numbers of 8.0 and 7.6, respectively. It is seen from Figure 10 that copper loss is faster at higher values of diffusion coefficient. The diffusion coefficients of copper possessing the value of 5×10^{-10} m^2 s^{-1} or less than that result in less efficient process with larger values of stabilization time. The diffusion coefficient also affects the overall mass transfer coefficient. The corresponding simulated values of overall mass transfer coefficient against diffusion coefficient are 4.33×10^{-6}, 2.78×10^{-6}, 0.97×10^{-6}, 0.61×10^{-6}, and 0.21×10^{-6} m s^{-1}. As discussed earlier, the diffusion coefficient of the solute is affected by temperature and viscosity and also varies for solute to solute, and it is a major factor which influences the mass transfer coefficient and hence affects the rate of solute extraction.

Effect of hydrodynamic conditions

Simulations were run to study copper extraction from initial concentration of 15.7 mol m^{-3} with oxime concentration of 77 mol m^{-3} under various hydrodynamic conditions of aqueous and organic phases. Different values of aqueous phase flow rates, for example, 5.0×10^{-6}, 8.3×10^{-6}, 12.5×10^{-6}, and 16.7×10^{-6} m^3 s^{-1}, were selected to study the copper extraction. These values correspond to Reynolds numbers in shell side of the HFMC of 3.2, 5.4, 8.0, and 10.7, respectively. The organic phase flow rate flowing in the fibers of HFMC is supposed to be constant at 6.7×10^{-6} m^3 s^{-1}, which corresponds to a Reynolds number of 7.6. Figure 11 shows that aqueous phase flow rate affects the initial velocity of extraction and faster extraction is achieved with larger values of aqueous phase flow rates, that is, process is stabilized in less time. Mass transfer resistance always lies on aqueous phase side (almost 97%). Simulated values of overall mass transfer coefficient are estimated as 1.11×10^{-6}, 1.5×10^{-6}, 1.91×10^{-6}, and 2.26×10^{-6} m s^{-1} with each value of aqueous phase flow rate, respectively. On the other hand, organic phase flow rate has nominal effect on copper extraction process.

As the resistance to mass transfer lies in aqueous phase boundary layer, increase in Reynolds number eases the solute mass transfer rate through this layer. However, we can notice that copper ions are more easily transferred than copper-oxime ions in their respective boundary layer. However, increase in Reynolds number does not increase the extent of copper extraction because the simulation is made at the same partition coefficient for all values of Reynolds numbers. Lin and Juang,[22] in their work to extract free and chelated Cu^{2+} from aqueous phase to an organic solution of

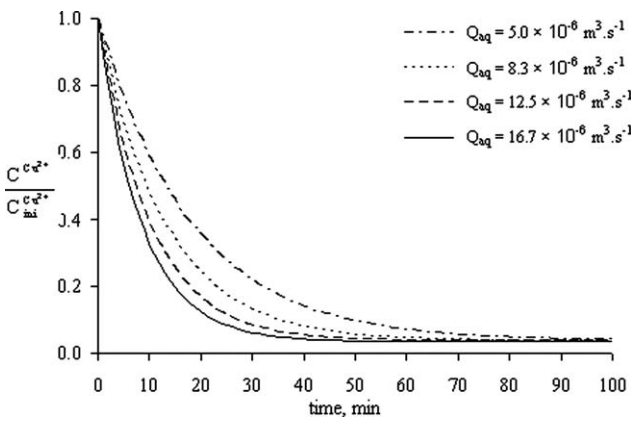

Figure 11. Effect of aqueous phase flow rate on extraction dynamics of copper with LIX 84-I.

LIX 64N and Aliquat 336 in HFMC, studied experimentally that the rate of extraction increases with decreasing flow rate of feed phase when the process is controlled by combined interfacial reaction and feed layer diffusion, but the flow rate of feed phase increases the extraction efficiency if the aqueous phase layer resistance is dominant in mass transfer. Breembroek et al.[30] studied the copper extraction in SLM with LIX 84-I and concluded that the aqueous phase layer was the limiting step, and so the increase of aqueous phase flow rate increases the rate of copper extraction.

Conclusions

Dispersion-free liquid–liquid copper extraction with LIX 84-I in a hydrophobic HFMC has been studied, theoretically and experimentally. Kinetic extraction and partition coefficients of copper ions with LIX 84-I oxime were measured in batch extraction, whereas nondispersive extraction was done in HFMC pilot unit. A mass transfer model of baffle-less module contactor, based on axial and radial approach, was developed considering steady-state diffusion mass transfer. This steady-state model was integrated with the dynamic model developed across storage tanks. The integrated model with the help of kinetic extraction data was scripted in MATLAB®, and simulations were run. The following results are highlighted,

(1) The reaction of copper ions with oxime was instantaneous at the interface, and resistance caused by the interfacial resistance has been ignored. Experimental results from batch extraction were verified with kinetic equation.

(2) Close agreement can be seen from the integrated dynamic model and experimental results for the concentration ranges and operating conditions studied. It allows predicting the process performance of the extraction unit under various kinetic and operating conditions.

(3) Efficient extraction is obtained for low copper feed concentration and with higher values of partition coefficient. Oxime concentration does not have a remarkable effect of the extraction. On contrary, high copper concentrated solutions are also extracted efficiently, for example, 83% of copper has been recovered when initial feed concentration was 31.5 mol m^{-3}. However, process was less efficient ($\leq$50%) for the partition coefficient (P) equal or less than 1.

(4) Aqueous phase diffusion dominates throughout the extraction process except for $P \leq 1$.

(5) Choice of extractant media, pH of aqueous phase, and temperature of the extraction system are proven to be parameters to improve partition coefficient and copper diffusivity and hence the efficiency.

(6) Aqueous phase flow rate and copper diffusivity do not influence the ultimate extraction efficiency, but with low values of aqueous phase flow rates and of copper diffusivity, process is stabilized in extended time. Stabilization time is independent of partition coefficient and copper feed concentration.

Notation

C = concentration, mol m^{-3}
C_1 = aqueous side (shell side) concentration, mol m^{-3}
C_2 = aqueous side (shell side) limiting layer concentration, mol m^{-3}
C_3 = organic side (fiber side) concentration in equilibrium with shell side limiting layer concentration, mol m^{-3}
C_4 = organic side (fiber side) limiting layer concentration, mol m^{-3}
C_5 = organic side (fiber side) concentration, mol m^{-3}
d = diameter, m
D = diffusivity, m^2 s^{-1}
J = mass transfer flux, mol s^{-1} m^{-2}
k = local mass transfer coefficient, m s^{-1}
K = overall mass transfer coefficient, m s^{-1}
L = fiber length, m
P = partition coefficient
Q = flow rate, cm^3 s^{-1}
R = mass transfer resistance, s m^{-1}
R_v = volume ratio, defined by Eq. 10
t = time, s
T = temperature, K
v = speed, m s^{-1}
V = volume, m^3

Greek letters

β = constant defined in Eq. 24
ε = porosity
Φ = extraction efficiency
γ = empirical factor defined by Eq. 1
Γ = time, defined by Eq. 35
η = viscosity, kg m^{-1} s^{-1}
κ = extraction equilibrium constant
ν = molar volume, cm^3 mol^{-1}
π = parachor, cm^3 $g^{1/4}$ $s^{-1/2}$
θ = packing fraction
ρ = density, kg m^{-3}
σ = membrane thickness, m
τ = tortuosity

Subscripts

aq = aqueous phase side
eq = equilibrium
ext = external
h = hydraulic
in = input
ini = initial
int = internal
lm = logarithmic mean
mb = membrane side
t = total
org = organic phase side
out = output

Superscripts

Cu^{2+} = ionic specie, copper ions
CuR_2 = ioinc specie, copper-oxime complex
H^+ = ionic specie, hydrogen ion
HR = ionic specie, oxime

Literature Cited

1. Johanson P. *Copper*, 1st ed. New York: The Rosen Publishing Group, 2007.
2. Fane AG, Awang AR, Bolko M, Macoun R, Schofield R, Shen YR, Zha F. Metal recovery from wastewater using membranes. *Water Sci Technol*. 1992;25:5–18.
3. Yu B, Zhang Y, Shukla A, Shukla SS, Dorris KL. The removal of heavy metal from aqueous solutions by sawdust adsorption-removal of copper. *J Hazard Mater B*. 2000;80:33–42.
4. Chmielewski AG, Urbanski TS, Migdal W. Separation technologies for metals recovery from industrial wastes. *Hydrometallurgy*. 1997;45:333–344.
5. Merigold CR. *Copper extractants: modified and unmodified oximes, a comparison*. In: *Proceedings Annual Technical Seminar*. China: MID, CNNMIEC-Yunnan Company, BGRIMM, 1996.
6. Cox M. *Liquid-liquid extraction and liquid membranes in the perspective of the twenty-first century*. In: Aguilar M, editor. *Solvent*

Extraction and Liquid Membranes: Fundamentals and Applications in New Materials. New York: Taylor & Francis group, 2008:1–20.
7. Sutherland K. *Profile of the International Membrane Industry: Market Prospects to 2008*, 3rd ed. Oxford, U.K.: Elsevier Advanced Technology, 2004.
8. Farajzadeh MA, Bahram M, Zorita S, Mehr BG. Optimization and application of homogeneous liquid-liquid extraction in preconcentration of copper(II) in a ternary solvent system. *J Hazard Mater*. 2009;161:1535–1543.
9. De Haan AB, Bartels PV, De Graauw J. Extraction of metal ions from waste water: modelling of mass transfer in a supported liquid membrane process. *J Membr Sci*. 1989;45:281–297.
10. Basualto C, Poblete M, Marchese J, Ochoa A, Acosta A, Sapag J, Valenzuela F. Extraction of cadmium from aqueous solutions by emulsion liquid membranes using a stirred transfer cell contactor. *J Braz Chem Soc*. 2006;17:1347–1354.
11. Valenzuela F, Basualto C, Tapia C, Sapag J. Application of hollow-fiber supported liquid membranes technique to the selective recovery of a low content of copper from a Chilean mine water. *J Membr Sci*. 1999;155:163–168.
12. Sengupta B, Bhakhar MS, Sengupta R. Extraction of copper from ammonical solutions into emulsion liquid membranes using LIX 84-I. *Hydrometallurgy*. 2007;89:311–318.
13. Lee KH, Evans DF, Cussler EL. Selective copper recovery with two types of liquid-membranes. *AIChE J*. 1982;24:860–868.
14. Lin S-H, Juang R-S. Mass-transfer in hollow-fiber modules for extraction and back-extraction of copper(II) with LIX 64N carriers. *J Membr Sci*. 2001;88:251–262.
15. Iversen SB, Bhatia VK, Dam-Johansen K, Jonsson G. Characterisation of micro-porous membranes for use in membrane contactors. *J Membr Sci*. 1997;130:205–217.
16. Kiani A, Bhave RR, Sirkar KK. Solvent extraction with immobilized interfaces in a microporous hydrophobic membrane. *J Membr Sci*. 1984;20:125–145.
17. Pabby AK, Sastre AM. *Hollow fiber membrane-based separation technology: performance and design perspectives*. In: Aguilar M, editor. *Solvent Extraction and Liquid Membranes*. New York: Taylor & Francis Group, LLC, 2008:91–140.
18. Yun CH, Prasad R, Guha AK, Sirkar KK. Hollow fiber solvent extraction: removal of toxic heavy metals from aqueous waste streams. *Ind Eng Chem Res*. 1993;32:1186–1195.
19. Kumar A, Haddad R, Alguacil FJ, Sastre AM. Comparative performance of non-dispersive solvent extraction using a single module and the integrated membrane process with two hollow fiber contactors. *J Membr Sci*. 2005;248:1–14.
20. Juang R-S, Huang H-L. Mechanistic analysis of solvent extraction of heavy metals in membrane contactors. *J Membr Sci*. 2003;213:125–135.
21. Juang R-S, Chen J-D, Huan H-C. Dispersion-free membrane extraction: case studies of metal ion and organic acid extraction. *J Membr Sci*. 2000;165:59–73.
22. Lin S-H, Juang R-S. Removal of free and chelated Cu(II) ions from water by a nondispersive solvent extraction process. *Water Res*. 2002;36:3611–3619.
23. De Gyves J, Hernandez-Andaluz AM, De San Miguel ER. LIX(R)-loaded polymer inclusion membrane for copper(II) transport 2. Optimization of the efficiency factors (permeability, selectivity, and stability) for LIX(R) 84-I. *J Membr Sci*. 2006;268:142–149.
24. Poling BE, Prausnitz JM, O'connell JP. *The Properties of Gases and Liquids*, 5th ed. New York: McGraw-Hill, 2001.
25. Flett DS, Okuhara DN, Spink DR. Solvent extraction of copper by hydroxyoximes. *J Inorg Nucl Chem*. 1973;35:2471–2487.
26. Baba Y, Iwakuma M, Nagami H. Extraction mechanism for copper (II) with 2- hydroxy-4-n-octyloxybenzophenone oxime. *Ind Eng Chem Res*. 2002;41:5835–5841.
27. Carter SP, Freiser H. Kinetics and mechanism of the extraction of copper with 2-hydroxy-5-nonylbenzophenone oxime. *Anal Chem*. 1980;52:511–514.
28. Uribe IO, Gulias JAI. *Modelling and optimization in solvent extraction and liquid membrane processes*. In: Aguilar M, editor. *Solvent Extraction and Liquid Membranes*. New York: Taylor & Francis Group, LLC, 2008:201–224.
29. Baudot A, Floury J, Smorenburg HE. Liquid-liquid extraction of aroma compounds with hollow fiber contactor. *AIChE J*. 2001;47:1780–1793.
30. Breembroek GRM, Straalen AV, Witkamp GJ, Rosmalen GMV. Extraction of cadmium and copper using hollow fiber supported membranes. *J Membr Sci*. 1998;146:185–195.
31. Viladomat FG, Souchon I, Pierre FX, Marin M. Liquid-liquid and liquid-gas extraction of aroma compounds with hollow fibers. *AIChE J*. 2006;52:2079–2088.
32. Bocquet S, Viladomat FG, Nova CM, Sanchez J, Athes V, Souchon I. Membrane-based solvent extraction of aroma compounds: choice of configurations of hollow fiber modules based on experiments and simulation. *J Membr Sci*. 2006;281:358–368.
33. Younas M, Druon Bocquet S, Sanchez J. Extraction of aroma compounds in a HFMC: dynamic modelling and simulation. *J Membr Sci*. 2008;323:386–394.
34. Hu Shih-Yao B, Wiencek JM. Emulsion-liquid-membrane extraction of copper using a hollow-fiber contactor. *AIChE J*. 1998;44:570–581.
35. Hu Shih-Yao B, Wiencek JM. Copper-LIX 84 extraction equilibrium. *Sep Sci Technol*. 2000;35:469–481.
36. Komasawa I, Otake T. The effects of diluent in the liquid-liquid extraction of copper and nickel using 2-hydroxy-5-nonylbenzophenone oxime. *J Chem Eng Jpn*. 1983;163:77–383.
37. Kuipa PK, Hughes MA. Diluent effect on the solvent extraction rate of copper. *Sep Sci Technol*. 2002;37:1135–1152.
38. Cheryan M. *Ultrafiltration and Microfiltration Handbook*, 2nd ed. New York: Technomic Publishing Co Inc, 1998.

Manuscript received Feb. 12, 2009, revision received Jun. 26, 2009, and final revision received Aug. 21, 2009.